Crystal Structure, Vibrational Spectroscopy and ab Initio Density Functional Theory Calculations on the Ionic Liquid forming 1,1,3,3-Tetramethylguanidinium bis{(trifluoromethyl)sulfonyl}amide

Rolf W. Berg,*,† Anders Riisager,†,‡ Olivier N. Van Buu,†,‡ Rasmus Fehrmann,†,‡ Pernille Harris,† Alina A. Tomaszowska,§ and Kenneth R. Seddon§

Department of Chemistry, Technical University of Denmark, Building 207, Kemitorvet, DK-2800 Kgs. Lyngby, Denmark, Centre for Catalysis and Sustainable Chemistry, Technical University of Denmark, Building 206, Kemitorvet, DK-2800 Kgs. Lyngby, Denmark, and The QUILL Centre, The Queen's University of Belfast, Stranmillis Road, BT9 5AG, Belfast, Northern Ireland, U.K.

Received: March 20, 2009; Revised Manuscript Received: April 29, 2009

The salt 1,1,3,3-tetramethylguanidinium bis{(trifluoromethyl)sulfonyl}amide, $[((CH_3)_2N)_2C{=}NH_2]^+[N(SO_2CF_3)_2]^-$ or [tmgH][NTf_2], easily forms an ionic liquid with high SO_2 absorbing capacity. The crystal structure of the salt was determined at 120(2) K by X-ray diffraction. The structure was found to be monoclinic, space group $P2_1/n$ with $a = 11.349(2)$, $b = 11.631(2)$, $c = 11.887(2)$ Å, and $\beta = 90.44(3)°$. Raman and IR spectra are presented and interpreted. The results are interpreted using ab initio quantum mechanics calculations that also predicted vibrational spectra. The relationship between the transoid (C_2 symmetry) structure of the $[NTf_2]^-$ ion and the conformationally sensitive bands is discussed.

Introduction

Room temperature ionic liquids are salts composed of organic or inorganic ions that are fluids at or close to room (ambient) temperature.[1,2] The stability, nonflammability, amphiphilicity, low volatility, and other characteristics of ionic liquids make them useful, inter alia, as solvents or alternative reaction media. In addition, they offer the intriguing possibility to tune their physical properties simply by changing the anion and/or cation, though comprehensive studies have been relatively scarce.

One rather new class of ionic liquids is based on the 1,1,3,3- or *N*,*N*,*N*′,*N*′-tetramethylguanidinium $(C_5H_{14}N_3)^+$ (or $[((CH_3)_2N)_2C{=}NH_2]^+$ or $[tmgH]^+$) cation. The ionic liquid of that cation and the bis{(trifluoromethyl)sulfonyl}amide anion, $[C_2F_6NO_4S_2]^-$ (or $[N(SO_2CF_3)_2]^-$ or $[NTf_2]^-$), have been studied. (Alternative abbreviations used in the literature include $[(CF_3SO_2)_2N]^-$, $[Tf_2N]^-$, $[NTf_2]^-$, [TFSI]$^-$, [TFSA]$^-$, [BTA]$^-$. In this paper, we use the most commonly accepted $[NTf_2]^-$.) This ionic liquid with its air and moisture stability, is of considerable interest because of its use in battery electrolytes and as an extraction medium for the recovery of SO_2 and CO_2 from stack gases.[3,4] In our previous study, it was demonstrated that [tmgH][NTf_2] can physically absorb large amounts of gaseous SO_2 at ambient temperature and pressure. The absorbed SO_2 gas remains in the molecular state and can readily be desorbed from the ionic liquid. To get a better understanding of the reasons for the apparent affinity for this liquid to absorb the gases, a detailed study of [tmgH][NTf_2] applying methods such as X-ray crystallography was undertaken, combined with vibrational Raman spectroscopy and DFT-type ab initio molecular orbital calculations. These methods are known to be very powerful tools in the study of molecular structures and intermolecular interactions among ions.[1] The structure and spectra yield important information on spatial relationships and interactions, and it was hoped to gain a better understanding of the solution chemistry of the combination of $[tmgH]^+$ with $[NTf_2]^-$.

TABLE 1: Crystal Data of [tmgH][NTf_2]

Formula	$C_7H_{14}F_6N_4O_4S_2$, or $[C_5H_{14}N_3]^+[C_2F_6NO_4S_2]^-$
M_w/g mol^{-1}	396.34
crystal size/mm	0.1 × 0.1 × 0.1
crystal system	monoclinic
space group	$P2_1/n$ (No. 14, C_{2h}^5)
a/Å	11.349(2)
b/Å	11.631(2)
c/Å	11.887(2)
β/°	90.44(3)
V/Å^3	1569.0(5)
D_c/g cm^{-3}	1.678
D_m/g cm^{-3}	1.6(2)
temperature/K	120(2)
Z	4
F(000)	808
μ (Mo-K_α)/mm^{-1}	0.426
wavelength/Å	0.71073
absorption correction	none
θ range for data collection/°	2.45 to 27.96
no. of reflections	20408 (7125 independent)
reflections collected	$-14 \le h \le 14$ $-15 \le k \le 15$ $-15 \le l \le 15$
R(int)	0.0208
reflections, total and with $I > 2\sigma(I)$	3742 and 3512
no. of parameters	212
$R_1 = \sum\|\|F_0\|-\|F_c\|\|/\sum\|F_0\|$ for all reflections	0.0315
for those with $F_0^2 > 2\sigma(F_0^2)$	0.0298
$wR_2 = [\sum w(F_0^2 - F_c^2)^2/\sum wF_0^4]^{1/2}$ for all reflections	0.0828
for those with $F_0^2 > 2\sigma(F_0^2)$	0.0812
weight function, where $P = (F_0^2 + 2F_c^2)/3$	$w^{-1} = \sigma^2(F_0^2) + (0.0562P)^2 + 0.7789P$
goodness of fit	0.908
residual charge density/e$^-$ Å^{-3}	$-0.294 < \rho < 0.358$

* To whom correspondence should be addressed. E-mail: rwb@kemi.dtu.dk. Tel: +45 45 25 24 12. Fax: +45 45 88 31 36.

† Department of Chemistry, Technical University of Denmark.

‡ Centre for Catalysis and Sustainable Chemistry, Technical University of Denmark.

§ The Queen's University of Belfast.

10.1021/jp902745j CCC: $40.75
Published on Web 06/09/2009

TABLE 2: Selected Bond Distances and Angles in the $[tmgH]^+$ Cation, in the Structure of $[tmgH][NTf_2]$, and Comparable Data

distance/angle	X-ray, this work at 120(2) K	ab initio[a] calculated[16]	[tmgH]Cl[13]	$[tmgH][H_2PO_4]$[14]	tmg·GaH_3[15]
N1−C1/Å	1.3408(15)	1.3475	1.3304(15)	1.3198(13)	1.316(3)
N3−C1/Å	1.3433(15)	1.3440	1.3417(15)	1.3451(14)	1.347(3)
N2−C1/Å	1.3393(15)	1.3440	1.3370(14)	1.3447(15)	1.360(3)
N1−H1A/Å	0.8600	1.0073	0.918(17)	0.88	0.78(3)
N1−H1B/Å	0.8600	1.0073	0.886(17)	0.88	
N2−C2/Å	1.4686(16)	1.4717	1.4630(17)	1.466(2)	1.455(3)
N2−C3/Å	1.4684(16)	1.4702	1.4543(15)	1.455(2)	1.457(3)
C2−H to C5−H/Å	0.9600	1.0900	0.98(1)	0.98	0.92(4) to 1.01(4)
N3−C4/Å	1.4635(16)	1.4702	1.4580(15)	1.461(2)	1.458(3)
N3−C5/Å	1.4693(15)	1.4717	1.4621(14)	1.458(2)	1.448(3)
N2−C1−N1/°	119.46(11)	119.13	120.91(10)	120.22(10)	120.21(19)
N2−C1−N3/°	121.25(11)	121.74	119.36(10)	119.01(10)	117.64(19)
N1−C1−N3/°	119.28(11)	119.3	119.70(10)	120.78(11)	122.15(19)
C1−N1−H1A/°	120.0	121.29	118.3(9)	120.0	112.6(23)
C1−N1−H1B/°	120.0	121.29	120.8(11)	120.0	
H1A−N1-H1B/°	120.0	117.4	119.5(14)	120.0	
C1−N3−C4/°	120.96(10)	121.44	122.60(9)	120.91(10)	121.9(2)
C1−N3−C5/°	122.42(10)	122.33	122.79(10)	121.53(12)	120.8(2)
C4−N3−C5/°	114.63(10)	115.27	114.45(9)	114.50(12)	114.9(2)
C1−N2−C3/°	122.21(11)	121.44	121.63(10)	121.27(11)	122.5(2)
C1−N2−C2/°	120.49(10)	122.33	121.51(10)	121.02(12)	120.8(2)
C3−N2−C2/°	115.64(10)	115.27	115.76(10)	115.34(12)	115.9(2)
angles around C2, C3, C4, C5/°	109.5	109(2)	109.5	109.5	104.0(3) to 113.2(2)

[a] Gaussian 03W DFT/B3LYP/6-311+G(d,p), energy for $[tmgH]^+ = -363.10735630$ au, dipole moment = 1.4001 D, and no imaginary frequencies.

Experimental Section

Synthesis. $[tmgH][NTf_2]$ was prepared from a solution of tmg (0.10 mol 1,1,3,3-tetramethylguanidine, 99%, Aldrich) in ethanol (100 mL) and an aqueous acidic solution of $HNTf_2$ (0.10 mol) in water (50 mL), obtained by cation exchange of $Li[NTf_2]$ (Aldrich), on hydrogenated Dowex 50 W × 2 resin (Aldrich). Caution: The direct neutralization of the strong base with the strong acid is highly exothermic and should be performed carefully, wearing eye protection, and stirring and cooling the solution in an ice bath. After continuous stirring (25 °C, 24 h), the solvent was removed under reduced pressure (1 mbar) at 70 °C, followed by heating in vacuo (0.1 mbar), leaving a nearly quantitative yield.[4] The raw product was recrystallized from ethanol/diethyl ether (1:3 v/v) mixture, followed by drying in vacuo (50 °C, 0.1 mbar) to produce a white solid. The melting point (T_m = 50 °C) was determined by differential scanning calorimetry using a TA-2620 DSC equipped with cryostat cooling (ca. 10 mg sample, 5 °C min^{-1} heating and cooling rates, see Supporting Information). By visual observation, the melting point was ca. 42−43 °C. Crystals suitable for X-ray measurements were grown from the melt in a freezer at −18 °C.

NMR spectra ($CDCl_3$, 25 °C) were recorded on a Bruker AM360 NMR spectrometer to characterize the compound, giving peak positions at ^1H NMR (300 MHz): δ/ppm = 3.01 (s, 12H; CH_3), 6.20 (s, 2H; NH_2). ^{13}C NMR (75.5 MHz): δ/ppm = 39.62 (N−CH_3), 122.08 (CF_3), 161.38 (N=C). Peak positions were determined relative to the solvent ($CDCl_3$: δ_H = 7.26 ppm, δ_C = 77.0 ppm).

X-ray Diffraction. Because of the low melting point, the crystals were mounted in a cold room using a cryo loop based on liquid dinitrogen. The crystal was transferred directly to liquid dinitrogen, where it was stored until it was mounted under the cryo stream at the diffractometer. Profile data from ω-2θ scans were collected at 120 K on a Bruker SMART CCD platform diffractometer[5] using graphite monochromated Mo Kα radiation. Data collection and reduction was performed using the SMART and SAINT systems.[5] SHELXTL software[6] was used to solve the structure by direct methods and refine it by weighted full-matrix least-squares fitting to F^2 using all data. Hydrogen atoms were observed and modeled at ideal positions (at distances 0.96 and 0.86 Å for CH and NH, respectively). Data collection and refinement details are given in Table 1. Positional and equivalent isotropic thermal parameters are listed in Supporting Information. Some selected bond lengths and angles are included in Tables 2 and 3.

Raman Spectroscopy. Dispersive DILOR-XY and Bruker-IFS66 FRA-106 Fourier-Transform Raman spectrometers were used as described elsewhere.[7−10] The FT-Raman spectrum for the solid sample and liquids were obtained on the Bruker spectrometer using a 1064 nm NIR Nd:YAG laser (<100 mW) and a liquid dinitrogen cooled Ge-diode detector, directly on a little capped glass tube. More than 400 scans were collected in a 100−3500 cm^{-1} (Stokes) range at approximately 23 °C. The resulting spectra were averaged, followed by apodization and fast-Fourier-transformation to obtain a resolution of ∼2 cm^{-1} and a precision better than 1 cm^{-1}. The spectra were not corrected for (small) intensity changes in detector response versus wavelength.

The dispersive Raman spectra of the gas phase were collected separately in sealed glass vials using a visible green light laser (533 nm doubled Nd-YVO_4) with nominal power up to 2 W. The spectra were recorded in several overlaid sections that were combined after removal of cosmic spikes. A broad fluorescent background was subtracted when necessary. The wavelength scales were calibrated with use of cyclohexane to a precision of about 1 cm^{-1}.[11]

Infrared Absorption. The infrared spectrum was recorded at room temperature from polycrystalline sample on a PerkinElmer Spectrum 100 FT-IR instrument using the Universal diamond ATR top plate (8 scans). The IR spectral resolution was ∼4 cm^{-1}.

Ab initio Calculations. The ab initio quantum chemical MO calculations were performed by use of a GAUSSIAN 03W program package[12] on a 3 GHz Pentium R4 computer operated under Windows XP. Guessed geometries of the molecular ions,

TABLE 3: Selected Bond Distances and Angles in the Transoid $[NTf_2]^-$ Anion, in the Structure of [tmgH][NTf_2], and Comparable Data

distance/angle	X-ray, this work at 120(2) K	ab initio[a] calculated	1,2,3-triethylimidazolium salt[19]	[C_2mim] salt[20] (2 ions)
N4−S1/Å	1.5831(11)	1.6117	1.568(3)	1.567(17), 1.578(15)
N4−S2/Å	1.5796(11)	1.6117	1.573(3)	1.564(16), 1.570(15)
S1−O1/Å	1.4282(11)	1.4615	1.421(3)	1.411(12), 1.413(14)
S1−O2/Å	1.4360(10)	1.4609	1.421(3)	1.402(18), 1.407(14)
S2−O4/Å	1.4294(11)	1.4609	1.421(3)	1.413(15), 1.440(12)
S2−O3/Å	1.4377(10)	1.4615	1.425(3)	1.420(14), 1.436(16)
S1−C6/Å	1.8383(14)	1.8956	1.829(4)	1.72(2), 1.78(2)
S2−C7/Å	1.8371(14)	1.8956	1.833(4)	1.83(2), 1.830(19)
C6−F2/Å	1.3283(15)	1.3387	1.324(4)	1.37(3), 1.35(2)
C6−F1/Å	1.3273(17)	1.3467	1.316(4)	1.33(2), 1.34(2)
C6−F3/Å	1.3330(15)	1.3411	1.329(4)	1.33(2), 1.33(2)
C7−F4/Å	1.3270(16)	1.3387	1.318(4)	1.27(3), 1.288(19)
C7−F5/Å	1.3290(18)	1.3467	1.325(5)	1.27(3), 1.28(3)
C7−F6/Å	1.3284(16)	1.3411	1.319(4)	1.32(2), 1.36(2)
S2−N4−S1/°	124.27(7)	126.44	124.77(17)	127.5(12), 125.9(11)
O1−S1−O2/°	118.52(7)	118.97	118.0(2)	118.4(9), 117.7(9)
O1−S1−N4/°	116.96(6)	117.32	116.91(17)	114.5(9), 108.0(8)
O2−S1−N4/°	108.05(6)	108.18	108.5(2)	109.4(9), 116.9(8)
O1−S1−C6/°	104.65(6)	104.27	104.16(17)	103.8(10), 102.6(10)
O2−S1−C6/°	103.39(6)	103.19	104.44(19)	105.0(12), 105.2(11)
N4−S1−C6/°	103.07(6)	102.38	102.63(17)	104.1(9), 104.4(9)
O4−S2−O3/°	118.54(7)	118.97	118.9(2)	118.7(9), 118.3(10)
O4−S2−N4/°	109.00(6)	108.18	108.2(2)	107.1(9), 118.6(8)
O3−S2−N4/°	115.94(6)	117.32	116.12(17)	114.5(8), 109.7(10)
O4−S2−C7/°	104.19(7)	103.19	104.9(2)	104.2(11), 106.3(11)
O3−S2−C7/°	104.21(6)	104.27	104.20(19)	104.5(11), 102.7(8)
N4−S2−C7/°	102.85(6)	102.39	102.26(17)	106.6(8), 97.7(9)
F1−C6−S1/°	111.77(9)	111.57	111.2(2)	117(2), 116.6(17)
F2−C6−S1/°	110.54(9)	111.44	111.3(2)	114.8(16), 112.5(15)
F3−C6−S1/°	109.36(10)	109.64	110.2(3)	114.3(15), 111.9(15)
F1−C6−F2/°	108.33(12)	108.21	108.2(3)	105.2(17), 101.7(19)
F1−C6−F3/°	108.24(11)	108.03	108.5(3)	103(2), 109.7(18)
F2−C6−F3/°	108.52(11)	107.82	107.3(3)	101(2), 103.1(19)
F4−C7−S2/°	111.54(9)	111.57	110.7(3)	111(2), 115.3(16)
F6−C7−S2/°	109.15(10)	109.64	109.5(3)	107.5(14), 106.8(14)
F5−C7−S2/°	111.14(10)	111.44	111.2(3)	110.5(16), 111.6(13)
F4−C7−F6/°	108.45(12)	108.21	108.4(3)	112(2), 113(2)
F4−C7−F5/°	107.76(11)	107.82	108.1(3)	107(2), 105.8(18)
F6−C7−F5/°	108.71(12)	108.03	108.9(3)	108(2), 103.3(15)

[a] Gaussian 03W DFT/B3LYP/6-311+G(d,p), energy for transoid $[NTf_2]^-$ = −1827.61042054 au, dipole moment = 0.2572 D, and no imaginary frequencies.

assumed to be in hypothetical gaseous free states without any symmetry, were used as input. The total geometric/conformational energies were minimized by use of Hartree−Fock/Kohn−Sham density functional theory (DFT) procedures at a level of approximation limited by use of the restricted-spin Becke's three-parameter hybrid exchange functional (B3), Lee−Yang−Parr correlation and exchange functionals (LYP), and with Pople's polarization split valence Gaussian basis set functions, augmented with d- and p-type polarization functions and diffuse orbitals on non-hydrogen orbitals (B3LYP, 6-311+G(d,p)). The Gaussian 03W software was used as implemented with the modified GDIIS algorithm and tight optimization convergence criteria. The vibrational frequencies and eigenvectors for each normal mode were calculated without adjusting the force constants.

Results and Discussion

Crystal Structure. The structure of [tmgH][NTf_2] showed a nearly planar {CN_3} core in the $[tmgH]^+$ cation, Figure 1. The bond lengths and bond angles are given in Table 2, which also shows previously determined X-ray structural data for the following other tetramethylguanidinium compounds: the chloride,[13] the dihydrogenphosphate,[14] and an unusually strongly bound gallane adduct of tmg, $(Me_2N)_2CN(H)\cdot GaH_3$.[15] The geometrical data compare well to each other. Also in Table 2, data for the optimized structure (see Figure 2) of the $[tmgH]^+$ ion have been included,[16] obtained by use of the Gaussian 03W program.[12] Although small deviations are seen, it proves that a quite reasonable model structure for the $[tmgH]^+$ ion can be obtained by the DFT-B3LYP/6-311+G(d,p) modeling of the isolated ion.

With respect to the $[NTf_2]^-$ anion in the [tmgH][NTf_2] crystal, the bond lengths and bond angles are given in Table 3. As expected, the structure showed terminal CF_3 groups rotated around their S−N bonds, thus adopting the most common "transoid" C_2 symmetry conformation of the ion;[17,18] see Figures 1 and 2. In Table 3, representative examples of X-ray structural data for previously determined compounds containing the $[NTf_2]^-$ anion were included: 1,2,3-triethylimidazolium[19] and 1-ethyl-3-methylimidazolium[20] salts (the second one with two different anion conformations). We refer to the Cambridge Structural Database[21] for further structures. Also the data for the optimized C_2 symmetry $[NTf_2]^-$ structure obtained by use of the Gaussian 03W program[12] are presented. As for the anion, only small deviations between the calculated and experimental

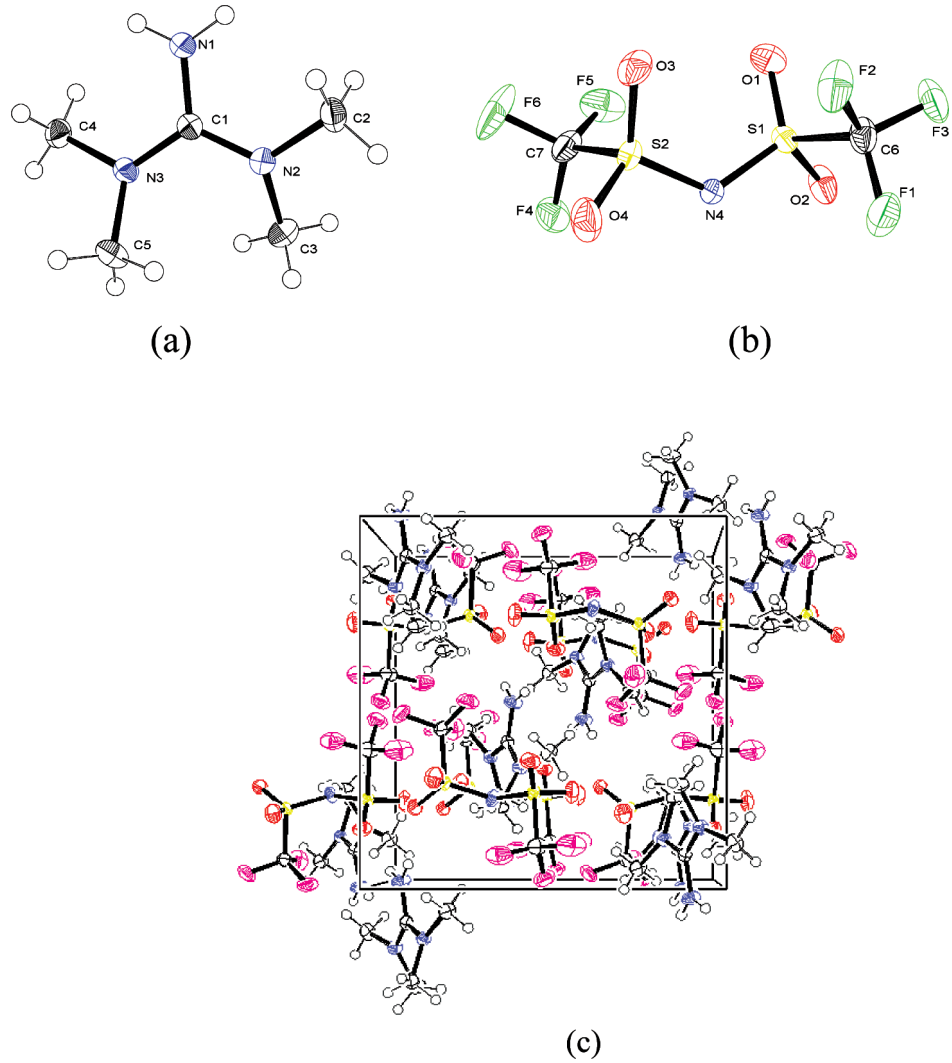

Figure 1. The structure of the $[tmgH]^+$ (a) and $[NTf_2]^-$ (b) ions and the crystal packing (c) showing a nearly planar $[tmgH]^+$ cation and a transoid conformation of the $[NTf_2]^-$ anion.

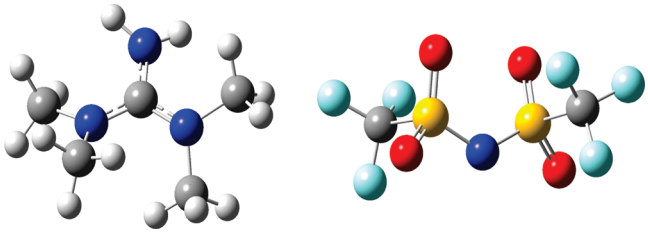

Figure 2. Optimized geometries of the $[tmgH]^+$ and $[NTf_2]^-$ ions, as obtained by DFT/B3LYP calculations with Gaussian 6-311G+(d,p) basis sets.

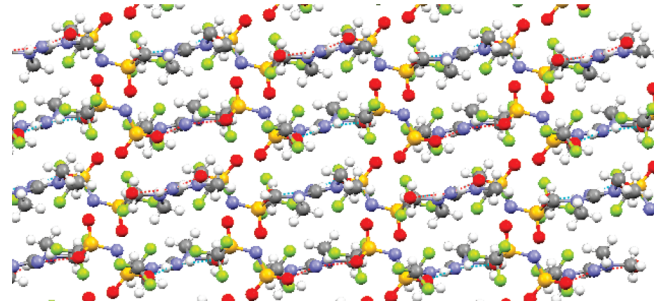

Figure 3. Layers in the structure of the $[tmgH][NTf_2]$ viewed along the *b* axis of the unit cell.

values are seen, once again proving good accordance with the DFT modeling.

The single crystal data revealed that in the structure of monoclinic $[tmgH][NTf_2]$, the cation is involved in close contact hydrogen-bonding interactions with two bistriflamide anions, forming infinite hydrogen-bonded layers (see Figure 3). The NH_2 group of the cation provides a hydrogen bond donating site to oxygens from two neighboring anions. The hydrogen−oxygen distances are 2.10 and 2.14 Å, well below the sum of their van der Waals radii (Figure 4).

Ab Initio Calculations. Molecular Orbital (MO) model calculations have recently become a quite efficient tool to predict chemical structures and vibrational (i.e. Raman scattering and IR emission) spectra. In previous work,[16] ab initio calculations on the isolated $[tmgH]^+$ ion were reported. Some of the calculated results are shown in Figure 2 and in Tables 2 and 3.

The bis{(trifluoromethyl)sulfonyl}amide anion, one of the more common anions forming room temperature ionic liquids, has been investigated by means of ab initio calculation numerous times.[22−29] The calculations were repeated here to see how the results compare with the experimental results and other models. We calculated equilibrium geometries and spectra of the isolated ions at the B3LYP/DFT/6-311+G(d,p) level by using the Gaussian 03W software,[12] neglecting anion−cation interactions.

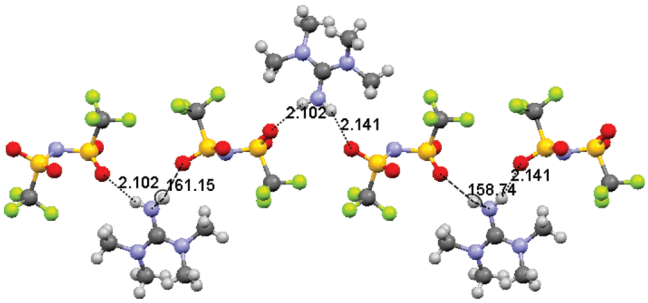

Figure 4. Lengths and angles of the N−H···O hydrogen bonds in the structure of [tmgH][NTf_2].

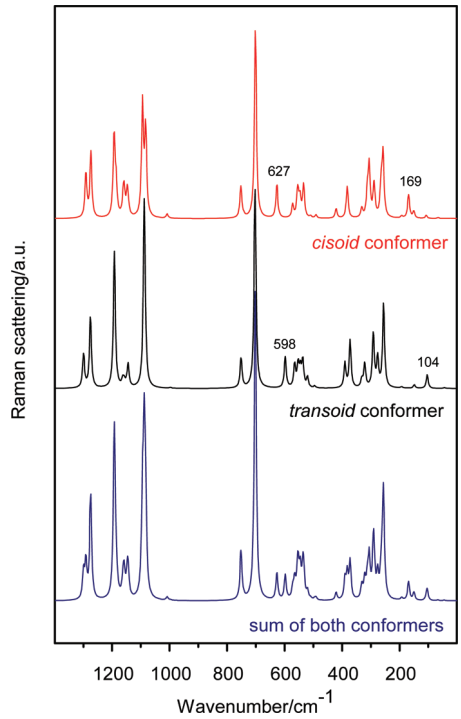

Figure 5. Calculated Raman spectra of the cisoid and transoid conformers of the $[NTf_2]^-$ ion and the sum of those spectra. The conformer ions have been calculated by DFT/6-311G+(d,p)/RB3LYP Gaussian modeling. Curves have been arbitrarily scaled and shifted.

The experimental bands were assigned to normal modes on the basis of potential energy distribution analysis.

According to the calculations on $[NTf_2]^-$ (prior to the normal frequency analyses), two conformers of C_2 and C_1 point group symmetry (a 2-fold rotational axis and minimal symmetry), respectively, were found to constitute global and local minima. The C_2 conformer was more favorable than the C_1 form. The energy levels were −1827.61042054 and −1827.60924174 au, respectively, not including the zero point energy corrections (0.052067 and 0.052063 au). The results of the geometric optimization for the C_2 conformer can be found in Table 3. The calculated spectra of both conformers are shown in Figure 5. A distinctive difference between the two conformers can be noticed, especially in the lower freqency region of the spectrum; the transoid conformation gives a band at around 598 cm^{-1} that is shifted to 627 cm^{-1} in the spectrum of the cisoid conformer. Our calculated results, some of which are summarized in Tables 4 and 5, are in overall agreement with results reported by Herstedt et al.[27,28] although we see some difference in intensities of the bands around 1090 cm^{-1}. Less distinctive differences in the spectra are hidden in the region near 300 cm^{-1}. The spectra of the two conformations are much alike, except for these small

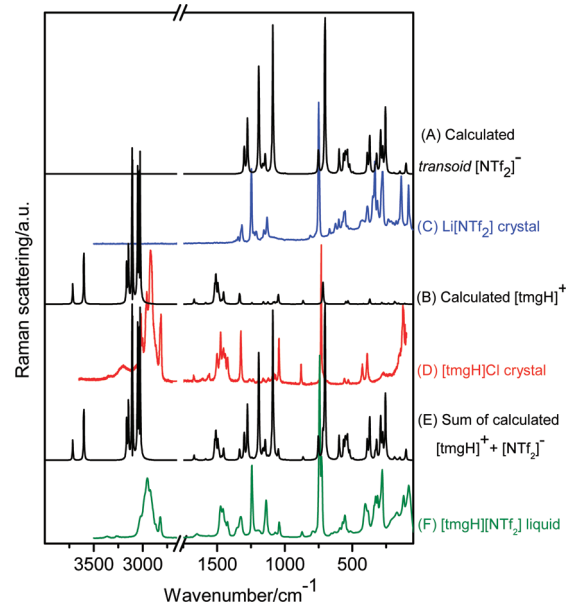

Figure 6. Illustrative example of the power of ab initio methods combined with Raman spectroscopy, applied on [tmgH][NTf_2] substance. The spectral curves (A) and (B) show calculated Raman spectra of minimized conformers of $[NTf_2]^-$ and $[tmgH]^+$ at the DFT/B3LYP/6-311+G(d,p) level compared to experimental spectra of the Li[NTf_2] (C) and [tmgH]Cl (D). The sum (shifted conveniently) of the calculated spectra is shown as curve (E), constituting a spectrum of a hypothetical [tmgH][NTf_2] liquid of noninteracting ions. (F) the experimental Raman spectrum of the liquid [tmgH][NTf_2].

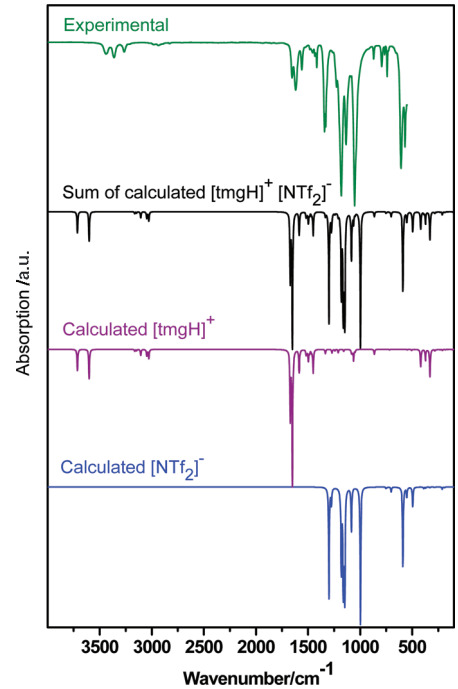

Figure 7. Experimental infrared absorption spectrum of crystalline [tmgH][NTf_2] (neat) compared to the individual spectra of the ions and their sum, calculated by the DFT/6-311G+(d,p)/B3LYP Gaussian modeling. Curves have been arbitrarily scaled and shifted.

differences in intensities and the splitting of the bands at 1080−1090 cm^{-1}.

Experimental Vibrational Spectra. The obtained Raman spectra of crystalline and liquid [tmgH][NTf_2] are compared to the calculated spectra of the free ions in Figure 6. On the basis of the crystallographic results, the transoid conformation of the $[NTf_2]^-$ anion was chosen as the preferred theoretical one (A)

TABLE 4: Calculated Vibrational Spectra for the $[tmgH]^+$ Ion and Assignments[16]

mode no.	wave number shifts/cm^{-1}	infrared absorption/km/mol	Raman activity/$Å^4$/AMU	depolarisation ratio	description of normal mode (Assigment)[a]
1	112.7	1.52	0.20	0.75	skeleton deformation
2	115.8	0.12	0.27	0.19	CN′ twist
3	160.0	0.52	0.55	0.57	CH_3 twist
4	182.2	1.53	0.65	0.75	CH_3 twist
5	190.9	0.11	1.85	0.41	CH_3 twist
6	212.4	4.36	0.14	0.75	CH_3 twist
7	237.4	1.38	0.70	0.75	CH_3 twist
8	268.4	1.12	0.33	0.61	CH_3 twist
9	282.7	5.24	1.14	0.32	NH_2 twist
10	329.0	105.24	0.25	0.75	NH_2 wag
11	372.0	0.03	2.98	0.23	symmetric N′C_2 deformation
12	375.1	41.31	0.86	0.75	NH_2 wag
13	423.1	78.48	0.22	0.75	NH_2 wag
14	504.6	4.46	0.16	0.75	NH_2 rock
15	536.4	0.01	2.86	0.17	NH_2 twist
16	548.7	1.73	1.82	0.35	CN'_2 bend
17	712.3	0.10	0.43	0.75	NH_2 rock + asymmetric N′C stretch
18	720.2	2.03	18.37	0.06	skeleton breathing
19	867.3	20.96	3.30	0.75	NH_2 rock + asymmetric N′C stretch
20	1052.3	8.58	9.68	0.38	CH_3 rock + CN_3 sym str
21	1065.8	43.91	1.17	0.75	NH_2 rock + CH_3 rock + N'C str
22	1079.0	12.80	1.77	0.72	CH_3 rock
23	1087.9	11.25	1.57	0.75	NH_2 rock + CH_3 rock + N′C str
24	1126.6	0.28	1.53	0.74	CH_3 def
25	1129.1	0.45	0.86	0.75	CH_3 def
26	1160.7	6.18	1.93	0.75	CH_3 def
27	1162.0	2.74	0.60	0.53	CH_3 def
28	1213.4	13.07	0.16	0.75	NH_2 rock + CH_3 rock + asym N′C str
29	1248.0	7.65	1.26	0.28	CH_3 rock + CN str + sym N′C str
30	1272.2	14.67	0.15	0.75	NH_2 rock + CH_3 rock + asym N′C str
31	1338.1	15.52	10.02	0.10	CN str + CN'_2 bend
32	1454.9	59.06	3.95	0.75	CH_3 asym umbrella
33	1457.1	15.12	12.22	0.61	CH_3 asym umbrella
34	1460.3	27.05	3.34	0.75	CH_3 asym umbrella
35	1473.1	9.99	2.87	0.08	CH_3 sym umbrella
36	1488.8	14.00	7.18	0.75	CH_3 def
37	1497.5	0.63	1.50	0.71	CH_3 def
38	1498.4	0.12	20.39	0.73	CH_3 def
39	1501.5	46.64	1.93	0.75	CH_3 def
40	1513.1	0.02	33.03	0.68	CH_3 def
41	1514.0	6.99	1.23	0.75	CH_3 def
42	1521.7	2.53	15.48	0.75	CH_3 def
43	1522.7	16.46	3.93	0.40	CH_3 def
44	1591.8	82.46	1.48	0.41	NH_2 sci + CN str
45	1660.5	532.13	1.02	0.75	CN'_2 asym str
46	1675.4	274.79	4.69	0.51	NH_2 sci + CN str
47	3042.9	31.43	19.69	0.75	CH_3 sym str
48	3043.2	8.62	276.80	0.05	CH_3 sym str
49	3059.1	12.19	14.59	0.75	CH_3 sym str
50	3061.8	20.61	354.74	0.02	CH_3 sym str
51	3124.1	6.09	186.47	0.68	CH_3 asym str
52	3124.5	15.89	41.81	0.75	CH_3 asym str
53	3128.3	0.85	45.69	0.75	CH_3 asym str
54	3128.4	0.66	41.96	0.28	CH_3 asym str
55	3165.5	2.99	63.07	0.75	CH_3 asym str
56	3165.6	1.86	29.85	0.75	CH_3 asym str
57	3183.5	7.07	34.62	0.75	CH_3 asym str
58	3183.6	0.21	28.04	0.71	CH_3 asym str
59	3609.6	117.02	90.63	0.11	NH_2 sym str
60	3731.1	81.26	38.37	0.75	NH_2 asym str

[a] N′ = N2 and N3. Abbreviations for approximate of vibration are the following: asym = asymmetric, bend = bending, def = deformation, rock = rocking, sci = scissoring, str = stretching, sym = symmetric, twist = twisting, wag = wagging.

for the comparison together with the theoretical spectrum of the $[tmgH]^+$ cation (B). These two ions gave calculated spectra that compared quite convincingly to those obtained for salts of monatomic counterions, that is, $Li[NTf_2]$ (C) and [tmgH]Cl (D). The $Li[NTf_2]$ spectrum has been obtained and assigned previously.[28,30,31] Note that the spectrum (D) could not be obtained in the range higher than 3500 cm^{-1} due to an instrumental limitation in the FT-Raman instrument. In Figure 6, also the sum of the calculated spectra of the $[tmgH]^+$ and $[NTf_2]^-$ ions is presented (E). This obtained sum corresponded

TABLE 5: Calculated Vibrational Spectra for the Transoid $[NTf_2]^-$ Ion and Assignments

mode no.	wave number shifts/cm^{-1}	infrared absorption/km/mol	Raman activity/Å^4/AMU	depolarisation ratio	description of normal mode (assigment)[a]
1	22.0	1.60	0.00	0.42	SO_2 twist + SCF_3 rock
2	37.4	0.27	0.00	0.32	CF_3 rock
3	43.7	1.71	0.00	0.75	SNS wag (whole skeleton def)
4	44.3	0.02	0.08	0.75	CF_3 rock
5	103.8	0.01	1.64	0.37	SNS twist
6	148.9	0.15	0.42	0.18	OSNSO sci
7	190.2	2.26	0.06	0.75	SO_2 twist + CF_2 twist
8	194.1	0.42	0.10	0.75	SO_2 twist + CF_2 twist
9	212.1	10.27	0.01	0.75	N wag + CF wag + SO_2 wag
10	255.6	0.14	10.50	0.23	CF wag + SO_2 wag
11	276.3	0.55	3.63	0.75	SO_2 rock + CF_3 twist
12	290.2	1.50	0.06	0.75	SC str ooph
13	291.3	0.05	6.76	0.74	CF wag + SO wag
14	321.2	0.09	3.07	0.31	SO rock + CF_3 twist
15	331.3	2.60	0.97	0.75	SNS wag + CF wag
16	372.0	5.18	6.04	0.23	OSNSO sci + CF_2 twist
17	390.0	7.31	3.16	0.75	SNS rock + CF_3 twist
18	495.3	90.85	0.26	0.75	SO_2 sci ooph + CF_2 sci
19	520.3	0.01	1.34	0.31	SO_2 sci + SNS sci + CF_3 rock
20	536.6	1.19	3.52	0.40	CF_2 sci + SNS sym str
21	545.0	0.73	2.26	0.75	CF_3 rock
22	553.0	45.36	2.94	0.75	CF_2 sci + SO_2 sci ooph
23	564.9	0.08	3.05	0.05	SO_2 wag iph + CF_3 def
24	589.2	375.21	0.04	0.75	SNS wag (whole skeleton def)
25	597.8	5.11	4.12	0.16	SNS sci (whole skeleton def)
26	702.7	22.97	28.08	0.01	SNS sym str + CF_3 umbrella iph
27	741.5	2.69	0.01	0.75	CF_3 umbrella ooph
28	751.4	6.22	4.14	0.12	CF_3 umbrella iph + SC str iph
29	997.8	627.24	0.10	0.75	SNS asym str + SO_2 sym str ooph + CF_3 sym str
30	1084.5	201.46	1.36	0.75	SO_2 str sym ooph + SNS asym str + CF str
31	1088.2	0.19	27.60	0.00	SO_2 sym str iph + CF_3 sym str iph
32	1144.2	161.15	3.36	0.18	CF_3 asym str
33	1149.0	424.53	0.38	0.75	CF_2 asym str + SO_2 sym str ooph
34	1157.9	197.41	0.90	0.71	CF_2 asym str
35	1163.3	405.37	1.04	0.75	CF_2 asym str
36	1180.8	385.19	0.02	0.75	CF asym str + SNS asym str
37	1192.2	9.35	20.87	0.39	CF_3 sym str iph + SO_2 sym str iph
38	1275.4	75.48	11.29	0.75	SO_2 asym str + SNS rock
39	1299.4	518.48	5.32	0.63	SO_2 asym str + SNS sci

[a] Abbreviations for approximate of vibration are the following: asym = asymmetric, bend = bending, def = deformation, iph = in-phase, ooph = out-of-phase, rock = rocking, sci = scissoring, str = stretching, sym = symmetric, twist = twisting, wag = wagging.

in coarse features to the spectrum of the liquid $[tmgH][NTf_2]$ compound (F), although some bands were shifted somewhat in position or intensity.

As explained previously, in many ab initio DFT studies when comparing calculated and observed bands (see, e.g., ref 32), one should not expect a perfect fit. Often the wavenumber (frequency) scale is calculated slightly too high due to the lack of good modeling of the orbitals and to model limitations in describing the internal and external interactions between the ions and the surroundings. In the present case, slight differences in frequencies, especially in the high-wavenumber end of the spectrum, can be noticed. Scaling factors might give a better agreement but none such was used in this work. Tables 4 and 5 thus show unscaled results. The assignments given in these Tables have been read off from the eigenvectors for the normal modes displayed on a computer screen to identify visually the dominating motions.

For the IR spectra of the $[tmgH][NTf_2]$, a similar situation was encountered when comparing the experimental and calculated results as presented in Figure 7. The experimental structural results were reproduced quite closely (within reasonable accuracy), proving again that a reasonable structure modeling is possible at the DFT-B3LYP/6-311+G(d,p) level. Typically, in ionic liquids, the constituent ions vibrate rather independently of the surroundings and therefore the liquid spectrum looks much like the sum of the solid salts, unless there are significant differences in hydrogen bonding pattern or ionic conformation between the two states. Thus, in presence of conformational equilibria, a closer study is worthwhile.

It is also interesting to compare the Raman spectra of $[tmgH][NTf_2]$ in the liquid and solid state. A small amount of the solid was placed in an ampule, melted, and measured at ~50 and ~25 °C in a supercooled liquid and in a glassy solid state. The obtained results are presented in Figure 8. Only small differences were observed between the spectra recorded. However, when comparing in detail to the spectra of the crystalline sample, noticeable differences can be observed; see Figure 9. In the liquid and glassy state spectra, additional bands appear at around 329 cm^{-1} whereas a band at 298 cm^{-1} of the crystal weakens. The bands from the liquid probably correspond to a mixture of the C_1 and C_2 conformers. We take bands at about 414, 397, 342, 317, 298, and 277 cm^{-1} to come from C_2 transoid $[NTf_2]^-$ ions, and bands at about 404, 340, 329, 280 and perhaps at around 354 cm^{-1} to originate from C_1 cisoid ions (at least partly). The observed reversal in the intensity ratio of the bands at around 410 and 390 cm^{-1} fits such an

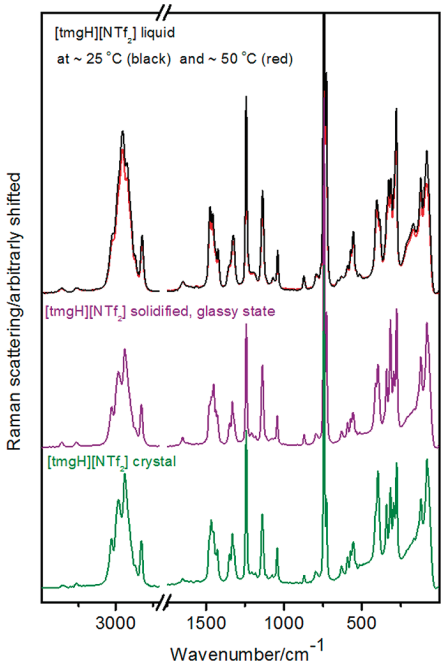

Figure 8. Experimental FT-Raman scattering spectra of liquid [tmgH][NTf_2] at two indicated temperatures, compared to the spectra of the solidified glassy state and the crystalline state. Spectral curves have been arbitrarily scaled and shifted.

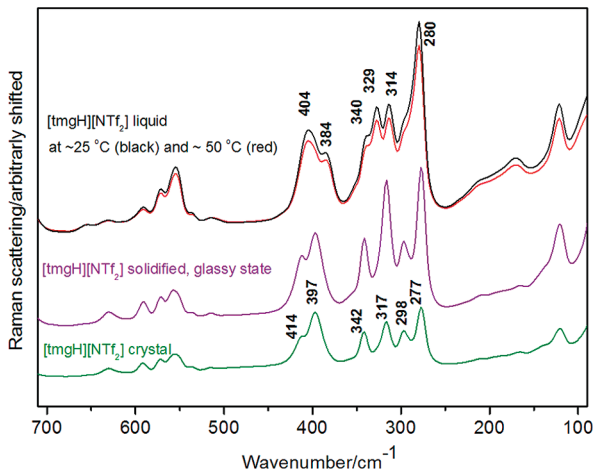

Figure 9. Detail of experimental FT-Raman scattering spectra of liquid [tmgH][NTf_2] at two indicated temperatures, compared to the spectra of the solidified glassy state and the crystalline state. Spectral curves have been arbitrarily scaled and shifted.

explanation. In Figure 10, strong bands in the cisoid and transoid conformers calculate to 382 and 373 cm^{-1}, respectively. From this, it is to be concluded that a conformational equilibrium exists between the C_1 and C_2 conformers of $[NTf_2]^-$ in liquid [tmgH][NTf_2]; after melting, about half of the ions of C_2 conformation must flip to C_1, and during crystallization the opposite must happen. This picture fits very well with results from other $[NTf_2]^-$ containing liquids[26,29] and with results by Trulove et al.[33] obtained during crystallization and melting of 1,3-dimethyl- and 1,2,3-trimethyl-imidazolium bis{(trifluoromethyl)sulfonyl}amide.

To see if the equilibrium remained in a glassy state, the liquid sample was immersed in liquid N_2, and another Raman spectrum recorded at room temperature (see Figure 8). Only small differences in the spectra were noticed. As mentioned before, the energy difference between the conformers of the bis{(trifluoromethyl)sulfonyl}amide ion is very small, thus making it likely that the equilibrium conformer distribution can be frozen in. Although the crystalline [tmgH][NTf_2] seems to exist only in the energetically favorable C_2 form, an equilibrium between both conformers is reached in the liquid phase and this can form a glassy state.

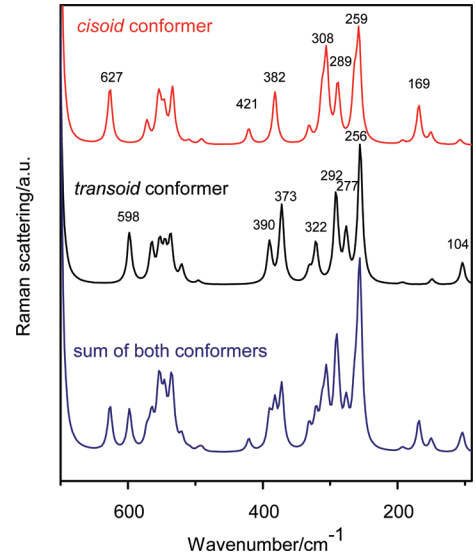

Figure 10. Detail of calculated Raman spectra of the cisoid and transoid conformers of the $[NTf_2]^-$ ion and the sum of those spectra. The conformer ions have been calculated by DFT/6-311G+(d,p)/B3LYP Gaussian modeling. Curves have been arbitrarily scaled and shifted.

Summary

A detailed study of the [tmgH][NTf_2] salt, based on crystallographic results combined with vibrational spectroscopy on the solid and the ionic liquid and on ab initio molecular orbital calculations, was undertaken. The obtained results, although not surprising, add weight to our understanding of the existence of mixtures of low symmetry conformers that disturb the crystallization process. The ab initio self-consistent quantum mechanical DFT functional methods with the chosen B3LYP/6-311+G(d,p) basis sets are well suited to reasonably model the molecular ion structures and calculate vibrational spectra of these ions. The results obtained indicated that neglecting the presence of cation−anion interactions is a reasonable approximation for a rather successful prediction of the Raman spectra. On the basis of such calculations, detailed and reliable assignments of the spectra are given and information on a conformational equilibrium obtained. It is shown that calculations on [tmgH][NTf_2] using the Gaussian 03W program converged to chemically reasonable results in quite close accordance with X-ray diffraction and Raman spectroscopy studies. The calculated results reproduced the experimental spectra in a satisfactory manner.

Acknowledgment. We wish to thank Professor Irene Shim (Department of Chemistry, DTU, Denmark) for help initiating the work. We are grateful to Lykke Ryelund (Chemistry Department, University of Copenhagen, Denmark) for recording FT Raman spectra. A grant from "Direktør Ib Henriksen's Fond" made maintenance of the Raman equipment possible and funding from the Lundbeck foundation (j.nr. 177/06), EPSRC (Portfolio Partnership Scheme, Grant EP/D029538/1), QUILL, and ESF is acknowledged.

Supporting Information Available: Figure showing the differential scanning calorimetry plot and two tables showing

fractional coordinates, equivalent and anisotropic thermal parameters for the atoms in [tmgH][NTf_2]. This material is available free of charge via the Internet at http://pubs.acs.org.

References and Notes

(1) Berg, R. W. *Monatsh. Chem.* **2007**, *138*, 1045–1075.

(2) Wasserscheid, P.; Welton, T. *Ionic Liquids in Synthesis*, 2nd ed.; Wiley-VCH: New York, 2008.

(3) Huang, J.; Riisager, A.; Wasserscheid, P.; Fehrmann, R. *Chem. Commun.* **2006**, *402*, 7–4029.

(4) Huang, J.; Riisager, A.; Berg, R. W.; Fehrmann, R. *J. Mol. Catal. A: Chem.* **2008**, *279*, 170–176.

(5) *SMART and SAINT, Area Detector Control and Integration Software*, version 5.054;Bruker Analytical X-ray Instruments Inc.: Madison, WI, 1998.

(6) Sheldrick, G. M. *SHELXTL, Structure Determination Programs*, version 6.12; Bruker Analytical X-ray Instruments Inc.: Madison, WI, 2001.

(7) Berg, R. W. In *Ionic Liquids in Chemical Analysis*; Koel, M., Ed.; CRC Press, Taylor & Francis Group: Boca, Raton, Florida, 2009; Chapter 12, pp 307−354.

(8) Berg, R. W.; Deetlefs, M.; Seddon, K. R.; Shim, I.; Thompson, J. M. *J. Phys. Chem. B* **2005**, *109*, 19018–19025.

(9) Brooker, M. H.; Berg, R. W.; von Barner, J. H.; Bjerrum, N. J. *Inorg. Chem.* **2000**, *39*, 4725–4730.

(10) Berg, R. W.; Maijó Ferré, I.; Cline Schäffer, S. J. *Vib. Spectrosc.* **2006**, *42*, 346–352.

(11) Berg, R. W.; Nørbygaard, T. *Appl. Spectrosc. Rev.* **2006**, *41*, 165–183.

(12) Frisch, M. J. Schlegel, H. B.; Scuseria, G. E.; Robb, M. A.; Cheeseman, J. R.; Montgomery, J. A., Jr.; Vreven, T.; Kudin, K. N.; Burant, J. C.; Millam, J. M.; Iyengar, S. S.; Tomasi, J.; Barone, V.; Mennucci, B.; Cossi, M.; Scalmani, G.; Rega, N.; Petersson, G. A.; Nakatsuji, H.; Hada, M.; Ehara, M.; Toyota, K.; Fukuda, R.; Hasegawa, J.; Ishida, M.; Nakajima, T.; Honda, Y.; Kitao, O.; Nakai, H.; Klene, M.; Li, X.; Knox, J. E.; Hratchian, H. P.; Cross, J. B.; Adamo, C.; Jaramillo, J.; Gomperts, R.; Stratmann, R. E.; Yazyev, O.; Austin, A. J.; Cammi, R.; Pomelli, C.; Ochterski, J. W.; Ayala, P. Y.; Morokuma, K.; Voth, G. A.; Salvador, P.; Dannenberg, J. J.; Zakrzewski, V. G.; Dapprich, S.; Daniels, A. D.; Strain, M. C.; Farkas, O.; Malick, D. K.; Rabuck, A. D.; Raghavachari, K.; Foresman, J. B.; Ortiz, J. V.; Cui, Q.; Baboul, A. G.; Clifford, S.; Cioslowski, J.; Stefanov, B. B.; Liu, G.; Liashenko, A.; Piskorz, P.; Komaromi, I.; Martin, R. L.; Fox, D. J.; Keith, T.; Al-Laham, M. A.; Peng, C. Y.; Nanayakkara, A.; Challacombe, M.; Gill, P. M. W.; Johnson, B.; Chen, W.; Wong, M. W.; Gonzalez, C.; Pople, J. A. *Gaussian 03W*, revision B.04; Gaussian, Inc.: Pittsburgh, PA; 2003.

(13) Fischer, A. K.; Jones, P. G. *Acta Cryst. E* **2002**, *58*, 218–219.

(14) Criado, A.; Diánez, M. J.; Pérez-Garrido, S.; Fernandes, I. M. L.; Belsley, M.; de Matos Gomes, E. *Acta Cryst. C* **2000**, *56*, 888–889.

(15) Cowley, A. R.; Downs, A. J.; Himmel, H.-J.; Marchant, S.; Parsons, S.; Yeoman, J. A. *Dalton Trans.* **2005**, 1591–1597.

(16) Berg, R. W.; Riisager, A.; Fehrmann, R. *J. Phys. Chem. A* **2008**, *112*, 8585–8592.

(17) Earle, M. J.; Hakala, U.; McAuley, B. J.; Nieuwenhuyzen, M.; Ramani, A.; Seddon, K. R. *Chem. Commun.* **2004**, *12*, 1368–1369.

(18) Deetlefs, M.; Hardacre, C.; Nieuwenhuyzen, M.; Padua, A. A. H.; Sheppard, O.; Soper, A. K. *J. Phys. Chem. B* **2006**, *110* (24), 12055–12061.

(19) Holbrey, J. D.; Matthew Reichert, W.; Rogers, R. D. *Dalton Trans.* **2004**, 2267–2271.

(20) Choudhury, A. R.; Winterton, N.; Steiner, A.; Cooper, A. I.; Johnson, J. K. *Cryst. Eng. Comm.* **2006**, *8*, 742–745.

(21) Allen, F. H. *Acta Cryst. B* **2002**, *58*, 380–388.

(22) Umebayashi, Y.; Fujimori, T.; Sukizaki, T.; Asada, M.; Fujii, K.; Kanzaki, R.; Ishiguro, S. *J. Phys. Chem. A* **2005**, *109*, 8976.

(23) Rey, I.; Johansson, P.; Lindgren, J.; Lassegues, J. C.; Grondin, J.; Servant, L. *J. Phys. Chem. A* **1998**, *102*, 3249.

(24) Johansson, P.; Gejji, S. P.; Tegenfeldt, J.; Lindgren, J. *Electrochim. Acta* **1998**, *43*, 1375–1379.

(25) Rey, I.; Lassegues, J. C.; Grondin, J.; Servant, L. *Electrochim. Acta* **1998**, *43*, 1505.

(26) Fujii, K.; Fujimori, T.; Takamuku, T.; Kanzaki, R.; Umebayashi, Y.; Ishiguro, S. *J. Phys. Chem. B* **2006**, *110*, 8179–8183.

(27) Herstedt, M.; Henderson, W. A.; Smirnov, M.; Ducasse, L.; Servant, L.; Talaga, D.; Lassègues, J. C. *J. Mol. Struct.* **2006**, *783*, 145–156.

(28) Herstedt, M.; Smirnov, M.; Johansson, P.; Chami, M.; Grodin, J.; Servant, L.; Lassègues, J. C. *J. Raman Spectrosc.* **2005**, *36*, 762.

(29) Lassègues, J. C.; Grodin, J.; Holomb, R.; Johansson, P. *J. Raman Spectrosc.* **2007**, *38*, 551–558.

(30) Brouillette, D.; Irish, D. E.; Taylor, N. J.; Perron, G.; Odziemkowski, M.; Desnoyers, J. E. *Phys. Chem. Chem. Phys.* **2002**, *4*, 6063–6071.

(31) Riisager, A.; Fehrmann, R.; Berg, R. W.; van Hal, R.; Wasserscheid, P. *Phys. Chem. Chem. Phys.* **2005**, *7*, 3052–3058.

(32) Sousa, S. P.; Fernandes, P. A.; Ramaos, M. J. *J. Phys. Chem. A* **2007**, *111*, 10439–10452.

(33) Trulove, P. C.; Henderson, W. A.; Reichert, W. M.; De Long, H. C.; Young, V. G., Jr.; Parsons, S.; Winterton, N. "Why are Ionic Liquids Liquid? The Importance of Ion Crystal Packing and Ion Disordering Mechanism", Book of Abstracts EUCHEM 2008 Conference on Molten Salts and Ionic Liquids, Copenhagen, Denmark, August 2008, Abstract O6-2, p. 40.

JP902745J